AFRL-SR-BL-TR-99-

0090

REPORT DOCUMENTATION PAGE

1. AGENCY USE ONLY *(Leave blank)*	2. REPORT DATE	3. REPORT TYPE AND DATES COVERED
	January 1999	Final Technical Report 15 Feb 95 to 30 Sep 98

4. TITLE AND SUBTITLE
Toughening of Heterogeneous Ceramics

5. FUNDING NUMBERS
F49620-95-1-0158

61102F
2302/BS

6. AUTHOR(S)
W. A. Curtin

7. PERFORMING ORGANIZATION NAME(S) AND ADDRESS(ES)
Engineering Science and Mechanics
Virginia Polytechnic Institute and State University
Blacksburg, VA 24060

8. PERFORMING ORGANIZATION REPORT NUMBER

9. SPONSORING/MONITORING AGENCY NAME(S) AND ADDRESS(ES)
Air Force Office of Scientific Research/NA
801 N. Randolph Street, Rm 732
Arlington, VA 22203-1977

10. SPONSORING/MONITORING AGENCY REPORT NUMBER
F49620-95-1-0158

11. SUPPLEMENTARY NOTES

12a. DISTRIBUTION AVAILABILITY STATEMENT
Approved for Public Release; Distribution Unlimited.

12b. DISTRIBUTION CODE
A

13. ABSTRACT *(Maximum 200 words)*

The goal of this program is to develop accurate micromechanical models of the damage mechanisms in fiber-reinforced composites, so as to provide predictive models of macroscopic composite behavior. Such predictive models clearly highlight the key controlling mechanisms of various stages of deformation and to quantitatively relate the constitutive properties of the fibers, matrix, and interface to the overall deformation of the composite. The understanding gained through such predictive models is then useful for optimizing material design and properties for various composite applications and for providing a baseline for studying issues such as composite degradation due to creep and time-dependent damage. Here, we summarize our progress in understanding three different phenomena in fiber-reinforced composites: the tendency of matrix cracks to deflect at a fiber/matrix as a function of the fiber and matrix elastic properties and the fiber and interface toughnesses; prediction of the stress-strain behavior of a ceramic composite as a function of elastic and stochastic strength properties of the fibers and matrix; and the dependence of tensile strength on fiber load transfer, including the size-scaling of strength.

14. SUBJECT TERMS	15. NUMBER OF PAGES
	13
	16. PRICE CODE

17. SECURITY CLASSIFICATION OF REPORT	18. SECURITY CLASSIFICATION OF THIS PAGE	19. SECURITY CLASSIFICATION OF ABSTRACT	20. LIMITATION OF ABSTRACT
UNCLASSIFIED	UNCLASSIFIED	UNCLASSIFIED	UL

Toughening of Heterogeneous Ceramics

Final Report

AFOSR GRANT #F94620-95-1-0158

February 15, 1995-September 30, 1998

W. A. Curtin, Principal Investigator
Division of Engineering, Brown University
Providence, RI 02912

worked performed at

Engineering Science and Mechanics
Virginia Polytechnic Institute and State University, Blacksburg, VA 24060

I. Introduction

The deformation and failure of fiber reinforced composites are controlled by a variety of damage mechanisms occurring at the fiber/matrix interface, in the matrix and fibers, and among fibers in the fiber bundle. The goal of this program was to develop accurate micromechanical models of these damage mechanisms to provide predictive models of macroscopic composite behavior. Such predictive models clearly highlight the key controlling mechanisms of various stages of deformation and to quantitatively relate the constitutive properties of the fibers, matrix, and interface to the overall deformation of the composite. The understanding gained through such predictive models is then useful for optimizing material design and properties for various composite applications and for providing a baseline for studying issues such as composite degradation due to creep and time-dependent damage. Considerable progress was made toward accomplishing these goals during the grant period; much of the work has been published in the literature, and references are provided at the end of this report. Of particular relevance are two major invited publications (References 1 and 2) that summarize much of the work of the Principal Investigator in this field. Here, we only summarize our progress in understanding three different phenomena in fiber-reinforced composites: the tendency of matrix cracks to deflect at a fiber/matrix; prediction of the stress-strain behavior of a ceramic composite; and the dependence of tensile strength on fiber load transfer.

II. Fiber/matrix Interface Debonding

Consider a matrix crack in a CMC that approaches the fiber/matrix interface (Figure 1). If the matrix crack penetrates and fails the fiber, then the composite is brittle. If the crack deflects at the interface, then the strength of the fibers can be accessed and strong, damage tolerant behavior can be obtained. Understanding the factors controlling deflection versus penetration is thus critical to the material design of CMCs. A crack will advance in a particular mode if the energy release rate G due to the crack advance is sufficient to pay the energy cost Γ of creating new crack area. The tendencies for deflection and penetration can thus be assessed by determining the respective energy release rates G_d and G_p and comparing these to the respective fracture energies Γ_i and Γ_f. At the interface between two materials of differing moduli, however, the energy release rates diverge or approach zero as the amount of crack advance (a_p into the fiber or a_d along the interface) approaches zero. Previous work by He and Hutchinson (HH) circumvented this issue by considering the ratio of G_d/G_p with $a_p=a_d$.[3] Their results for G_d/G_p versus the Dundur's parameter α (essentially $(E_f-E_m)/(E_f+E_m)$) are shown in Figure 2; deflection is predicted for $\Gamma_i/\Gamma_f < G_d/G_p$. However, for finite a_d,a_p and finite fiber volume fraction V_f, the G_d/G_p can be rather different than obtained by HH.

We have performed a set of calculations for the energy release rates G_d and G_p at finite V_f, finite a_d,a_p and in an axisymmetric geometry.[4] The calculations are performed using a model due to Pagano et al., which is an accurate, efficient method for determining stresses and energies for axisymmetric composites.[5] For small V_f=1% and small $a_d=a_p$=0.002r (r=fiber radius) our results for G_d/G_p are essentially identical to those obtained by HH. However, at V_f=40% and crack sizes $a_d=a_p$ ranging from 0.002r to 0.025r, we find much lower ratios of G_d/G_p, as shown in Figure 2. *Crack deflection is thus more difficult (requires less-tough interfaces) as both V_f and $a_d=a_p$ increase*

from zero; the HH prediction tends to be too optimistic in assessing prospects for crack deflection.

A group at WPAFB has fabricated model composites composed of SCS-0 SiC fibers and a glass matrix.[6] From the established matrix and fiber moduli and toughnesses, both α and the ratio of Γ_i/Γ_f can be determined, as shown in Figure 3. The HH criterion predicts crack deflection; our calculations predict crack penetration for a wide range of possible crack sizes $a_d=a_p$. The physical composites show brittle behavior and no evidence of fiber/matrix interface debonding. The observed behavior is thus consistent with our calculations (although our minimum values of a_d,a_p are determined by computational limitations not physical lengths).

Our results show a fairly strong dependence on the crack sizes a_d and a_p and raise some important conceptual issues. How are a_d and a_p physically interpreted? Are they atomistic lengths, lengths of some microstructural scales in the interface and fiber, or lengths of intrinsic cracks in the interface and fiber? The interpretation is uncertain but has an important implication for interface design. Specifically, if the conditions for interface debonding depend on some pre-existing physical defects then the engineering of interfaces must focus on controlling such defects. This is far more difficult than controlling the intrinsic fracture energies of potential interface coatings. More work must be done to properly resolve these issues.

III. Stress-Strain Behavior in CMCs

After debonding has successfully occurred at the fiber/matrix interface, the subsequent deformation of the composite is controlled by a residual sliding resistance τ across the interface. Furthermore, additional pre-existing matrix flaws can grow and become full-length matrix cracks, and pre-existing flaws in the brittle fibers can also extend across individual fibers. These cracking modes, and the associated slip at the fiber/matrix interface, lead to non-linear stress-strain behavior and ultimately to composite failure. Since the macroscopic σ-ε behavior is used for engineering design, it is important to fully understand its dependence on the properties of the fibers, matrix, and interface.

Both the matrix and fibers are intrinsically brittle materials, so their failures by cracking are determined by statistical distributions of flaws. The number of flaws per unit length combined with the interface sliding, which controls the amount of strain released per crack, determines the detailed shape of the stress-strain curve. We have recently developed models to predict the evolution of statistical matrix cracking, statistical fiber cracking and the associated stress-strain behavior, as a function of the fiber and matrix strength distributions, the elastic moduli, volume fractions, and interfacial τ in unidirectional CMCs.[7-9] The most recent models demonstrates an important transition in failure behavior.[8,9] For matrix strengths larger than the fiber bundle strength, there are few matrix cracks prior to composite failure and hence very little non-linear deformation and a small failure strain. For lower matrix strengths, more extensive matrix cracking occurs prior to failure, allowing for increasing non-linear deformation and larger failure strain. The failure strain increases until, for the weakest matrices, the failure strain is controlled entirely by the fibers. Predictions of this transition with decreasing matrix strain are shown in Figure 4 for a "typical" composite. Many of the micromechanical parameters entering the theory depend on the interfacial sliding resistance τ. The model provides predictions of the stress-strain

behavior expected as τ is varied while other parameters, such as fiber and matrix statistical flaw distributions and elastic constants, are held fixed. Changing τ can occur due to modified interface coatings or interface roughness with no other changes to the composite, and so is a feasible means of composite design. Figure 4 shows the predicted stress-strain behavior for a "tough" composite as τ is increased by multiples of 2, 4, and 8 over a baseline value. Although the tensile strength inceases monotonically with increasing τ, the composite failure strain does not increase. In fact, the failure strain can be non-monotonic. Such unusual behavior was previously unanticipated. From a design perspective, it is important to have both high matrix cracking stresses and large failure strain in CMCs. The present model shows the trade-offs maximizing these features of the deformation.

Application of the model to SiC/SiC "minicomposites" tested by Lissart and Lamon[10] shows excellent agreement with experiment when only the matrix strength parameters are adjusted (Figure 6).[8] These materials have fairly high matrix strengths and so (i) the failure strains are lower than the maximum possible values (which is 0.88% in this case) and (ii) matrix cracking is not fully saturated at the failure point. From the matrix strength parameters, fiber pullout lengths, and hysteretic behavior, three independent values for τ can be derived and all predict $\tau \approx 20$ MPa.

The broad capabilities of the model for predicting stress-strain behavior have yet to be fully exploited. We anticipate wide application of these results to various CMC systems, particularly as the manufacturing reliability of components from specific material systems becomes an issue. In such applications, the model may aid in identifying the source of relatively tough versus brittle behavior as a function of variations in manufacturing processes.

IV. Ultimate Tensile Strength

Most models for tensile strength assume that the load lost by broken fibers is transferred equally to all other fibers in the sample cross-section (Global Load Sharing, GLS). Although these models successfully predict the strength of many ceramic composites having low-τ interfaces, it is expected that, for higher-τ interfaces and MMC and PMC materials, the load transfer is much more local. The existence of Local Load Sharing (LLS) to any degree also implies that composite strength is sensitive to locally-damaged regions, is dependent on the physical composite size, and is statistically distributed. These features make composites weaker and more brittle, and thus must be clearly understood at a fundamental level to accurately predict composite behavior and to guide the design of composite components.

We have developed a new numerical model for calculating the tensile strength of a fiber-reinforced composite under LLS with the spatial extent of the load transfer being an adjustable parameter.[11,12] Numerical simulations of composite failure exhibit all of the features noted above, and particularly the scaling of strength with composite size.[11-17] From our simulation results, we have deduced some fascinating underlying scaling relations that actually relate the LLS problem to the analytically-tractable GLS problem.[12] We have also generalized the simulation model to incorporate "notches" or pre-existing cracks, free surfaces and edges, stress gradients, and "random" arrangements of the fibers.

Careful analysis of the LLS results combined with size-scaling concepts has lead to the development of a handy analytic model for predicting size-dependent composite

tensile strength under conditions of local load sharing. Our previous work has shown that the characteristic in-situ strength and gauge length for fibers in a composite are

$$\sigma_c = \left(\frac{\sigma_o^{\rho}\tau L_o}{r}\right)^{\frac{1}{1+\rho}} \quad ; \quad \delta_c = \frac{r\sigma_c}{\tau} = \left(\frac{\sigma_o r L_o^{1/\rho}}{\tau}\right)^{\frac{\rho}{1+\rho}} \tag{1}$$

where σ_o is the Weibull strength parameter at a reference gauge length L_o and ρ is the "Weibull modulus". r is the fiber radius and τ is the interfacial sliding. The characteristic length δ_c is the statistical analog of the "ineffective" length that has been widely used in many theories of composite strength. All lengths and strengths in the theory are naturally normalized by these two values, respectively. Now consider a composite consisting of n_f fibers and physical length L, with fibers having a Weibull modulus ρ. There is a critical damage cluster responsible for failure that consists of n_l fibers, where

$$n_l = 403\rho^{-1.28} \quad , \tag{2}$$

and having longitudinal length $0.4\delta_c$. The strength distribution for the critical cluster is a Gaussian distribution, and the mean strength $\mu^*_{n_l}$ and standard deviation $\gamma^{**}_{n_l}$ (normalized by σ_c) for the appropriate sizes n_l are given in Table I. The full composite can then be considered as a collection of mn "links" of the basic critical-size cluster, with

$$m=L/0.4\delta_c \quad ; \quad n=n_f/n_l \quad . \tag{3}$$

The cumulative probability of failure for the full composite is predicted to be a Weibull distribution,

$$H_{mn}(\sigma) = 1 - e^{\left(\frac{\sigma}{\tilde{\sigma}_{mn}}\right)^{\tilde{\rho}}} \quad , \tag{4}$$

where the characteristic composite tensile strength $\tilde{\sigma}_{mn}$ and Weibull modulus $\tilde{\rho}$ are given by

$$\tilde{\sigma}_{mn} = \mu^*_{n_l} - \gamma^{**}_{n_l}\left[\sqrt{2\ln(mn)} - \frac{\ln(\ln(mn)+\ln(4\pi)}{\sqrt{8\ln(mn)}}\right] \tag{5}$$

$$\tilde{\rho} = \frac{\tilde{\sigma}_{mn}}{\gamma^{**}_{n_l}}\sqrt{2\ln(mn)} \quad . \tag{6}$$

The measured composite strength in non-dimensional form is

$$\sigma_{uts} = f\sigma_c\tilde{\sigma}_{mn} + (1-f)\sigma_m \tag{7}$$

where f is the volume fraction of fibers and σ_m is the load carried by the matrix at failure. Figure 7 shows a comparison of the strength vs. composite size as predicted by Eqs. 2-7

and as obtained via the LLS simulations; the agreement is excellent over many orders of magnitude in composite size.

m	n_l	$\mu^*_{n_l}$	$\gamma^*_{n_l}$
2.0	166	0.6869	0.0231
3.0	99	0.6996	0.0257
4.0	68	0.7256	0.0278
4.5	59	0.7415	0.0285
5.0	51	0.7442	0.0293
5.5	45	0.7516	0.0300
6.0	41	0.7595	0.0303
6.5	37	0.7676	0.0307
7.0	33	0.7760	0.0310
7.5	31	0.7832	0.0314
8.0	28	0.7909	0.0319
8.5	26	0.7979	0.0321
9.0	24	0.8047	0.0322
9.5	23	0.8106	0.0324
10.0	21	0.8173	0.0327

Table I. Critical link size n_l, mean link strength $\mu^*_{n_l}$ and link standard deviation $\gamma^{**}_{n_l}$, normalized by σ_c, for various fiber Weibull moduli ρ. These parameters are used in the analytic model of Eqs. 2-7.

As an example of the predictive capability of the model, we have applied the LLS model to predict the tensile strengths of various Ti-MMCs. The physical composites are actually sufficiently small that direct numerical simulation of the full composite is feasible. Input to the predictions are only constitutive information: the in-situ fiber strength distribution, fiber volume fraction, fiber diameter r, interfacial shear stress τ, and matrix yield strength σ_{my}. The predicted and measured strengths for Ti-1100 reinforced with SCS-6 fibers are shown in Table II, where the data are from the work of Gundel and Wawner.[18] Excellent agreement is obtained, which is typical of results obtained on other Ti-MMC materials.[14,15]

	Fiber Volume Fraction	In-situ Fiber strength @ 1"	Interface τ	UTS: expt.	UTS: theory
B	0.15	3930	190	1252	1341
C	0.18	4310	190	1300	1470
D	0.20	2890	190	1230	1353
F	0.26	4270	65	1496	1630
G	0.28	4640	65	1724	1768
H	0.30	3330	65	1327	1535
I	0.35	4410	80	1716	1929

Table II. Measured, predicted tensile strengths in Ti-1100 MMCs. All stresses in MPa.

Ramamurty et al. have recently taken the analytic theory and applied it to the prediction of strength in Aluminum matrix materials reinforced Nextel Alumina fibers.[19] With no adjustable parameters, the theory predictions are shown in Figure 8. The agreement is excellent, both in absolute magnitude and in the trend of decreasing strength with increasing size. Ramamurty et al. also demonstrated that the strength fluctuations at fixed composite size were due primarily to the fluctuations in average fiber volume fraction among the samples tested. The size-scaling of strength thus cannot be obtained by using a simple Weibull model relating the strength distribution at a single size to the average strength versus size.

We have also recently applied the model to predict the tensile strengths of several graphite/epoxy polymer matrix composites.[16,17] Proper application of the model requires accurate input data on fiber strengths and critical gauge lengths. These were obtained for the PMC materials through careful analysis of single fiber composite test data available in the literature but interpreted using a previously-developed model of the PI. Table III shows the constituent fiber strength properties and critical length, and the predicted composite tensile strength and failure strain. The predictions agree with the experiments to within 20%.[17] Part of the discrepancy may be due to the use of a single Weibull model, whereas data on Carbon fibers suggests a more complicated strength-length scaling relationship. In any case, size-scaling of the composite strength plays an important role in obtaining quantitative accuracy: using a Global Load Sharing model would yield predictions that were too large by 40% or more.

Material							σ_{uts}		σ_{uts}/E_c	
System	σ_c	δ_c	ρ	E_c	V_f	mn	Expt	Theo.	Expt	Theo.
AS-4/ 828mPDA	5783	501	10.7	138	0.59	1.5 x10^7	1890	2225	0.0137	0.0161
AS-4C/ 828mPDA	5863	458	10.7	150	0.64	1.6 x10^7	2044	2455	0.0137	0.0164
AS-4/ J2	5783	501	10.7	124	0.53	1.3 x10^7	1830	1998	0.0147	0.0161
AS-4CGP/ J2	5783	501	10.7	126	0.54	1.2 x10^7	1640	2036	0.0130	0.0161
T300/ Epincote	5436	378	7	232	1.00	1.2 x10^5	2880	3479	0.0124	0.0149
T300/ #3601	5181	378	7	138	0.59	1.0 x10^7	1575	1871	0.0114	0.0136
T300/ #3631	5436	378	7	136	0.59	1.0 x10^7	1740	1963	0.0128	0.0144

Table III. Constitutive and composite data for various systems, and measured and predicted tensile strengths. Th(f) denotes prediction using physical volume fraction; Th(f_e) denotes prediction using effective volume fraction. Data in parenthesis for T300 systems is obtained using estimated thermal stress corrections in the s.f.c. test. Units are as follows: σ_c(MPa), δ_c(μm), E_c(GPa), σ_{uts}(MPa).

To summarize, the numerical and analytical tools we have developed are predictive and demonstrate the detailed nature of fiber damage evolution expected in fiber-reinforced composites depending on the nature of the load transfer. These models will form the basis of future work on time-dependent damage evolution and notch sensitivity.

V. Summary

We have briefly discussed our major progress in understanding deformation and failure modes in fiber-reinforced composites. The models developed here show the subtle and specific connections between micromechanical constitutive properties and macroscopic measured quantities such as tensile strength and strain. Assessment of the models by detailed comparison with experiments demonstrates their accuracy. These models thus provide guidelines for material development and optimization of the fiber/matrix interface toughness, the fiber and matrix flaw sizes, the interfacial sliding resistance, and the load transfer among fibers. Furthermore, the models of quasistatic deformation and failure form the basis for the development of micromechanical models for time-dependent evolution of damage and ultimate failure including the phenomena of creep, interface evolution, and fiber degradation at elevated temperatures. Our future work is aimed at developing models for accurate life prediction of fiber-reinforced composites.

VI. Students and Post-doctoral associates supported under this contract

B. K. Ahn, PhD in Engineering Mechanics, December, 1997.

Glenn C. Foster, MS in Engineering Mechanics, February, 1997

M'hamed Ibnabdeljalil, Post-doctoral associate in Engineering Mechanics.

VII. References

(references in bold stem from the present project; reprints of all papers published under this contract are attached)

1. **W. A. Curtin, Advances in Applied Mechanics, 1999, 36:163.**
2. **W. A. Curtin, Stress-strain behavior in brittle matrix composites, to appear in Comprehensive Composite Materials, ed. Kelly and Zweben, 2000.**
3. M. Y. He and J. W. Hutchinson, Int. J. Solids & Structures, 1989, 25:1053.
4. **B. K. Ahn, W. A. Curtin, T. A. Parthasarthy, and R. E. Dutton, J. Comp. Sci. Tech., 1998, 58:1775.**
5. N. J. Pagano and H. W. Brown III, Composites, 1993, 24:69.
6. C. M. Gustafson, R. E. Dutton, and R. J. Kerans, J. Am. Cer. Soc., 1995, 78:1423.
7. **B. K. Ahn and W. A. Curtin, J. Mech. Phys. Solids, 1997, 45:177.**
8. **W. A. Curtin, B. K. Ahn, and N. Takeda, Acta Met., 1998, 46:3409.**
9. **W. A. Curtin, B. K. Ahn, and N. Takeda, Cer. Trans., 1998, 99:187.**
10. N. Lissart and J. Lamon, Acta Met. , 1997, 45:1025.
11. **S. J. Zhou and W. A. Curtin, Acta Met., 1995, 43:3093.**
12. **M. Ibnabdeljalil and W. A. Curtin, Intl. J. Solids & Structures, 1997, 34:2649.**
13. **M. Ibnabdeljalil and W. A. Curtin, Acta Met., 1997, 45:3641.**
14. **G. C. Foster, M. Ibnabdeljalil and W. A. Curtin, Intl. J. Sol. Str., 1997, 35:2523.**
15. **G. Foster, MS Thesis, VPI & SU, Blacksburg, VA, February, 1998.**
16. **W. A. Curtin and N. Takeda, J. Composite Materials, 1998, 32: 2042.**
17. **W. A. Curtin and N. Takeda, J. Composite Materials, 1998, 32:2060.**
18. D. Gundel and F. Wawner, Comp. Sci. Tech., 1997.
19. U. Ram, F. W. Zok, F. Leckie, and H. E. Deve, Acta Met., 1997, 45:4603 .

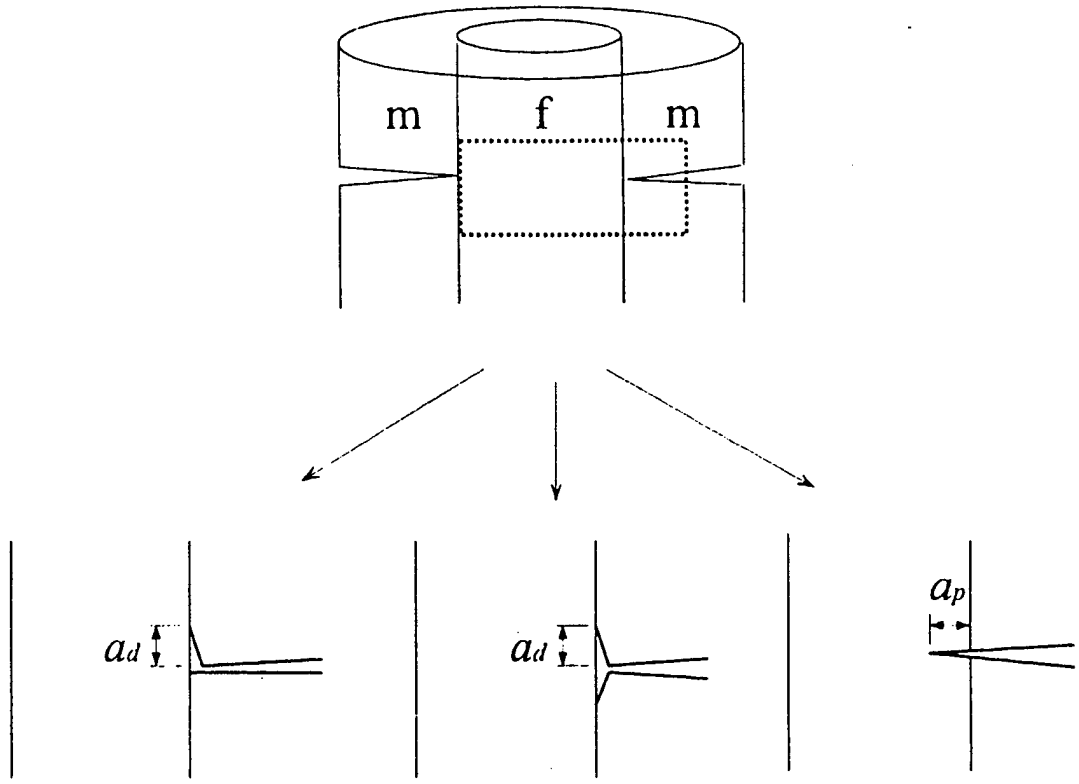

Singly deflected crack Doubly deflected crack Penetrated crack

Figure 1. Three possible modes of cracking at the fiber/matrix interface

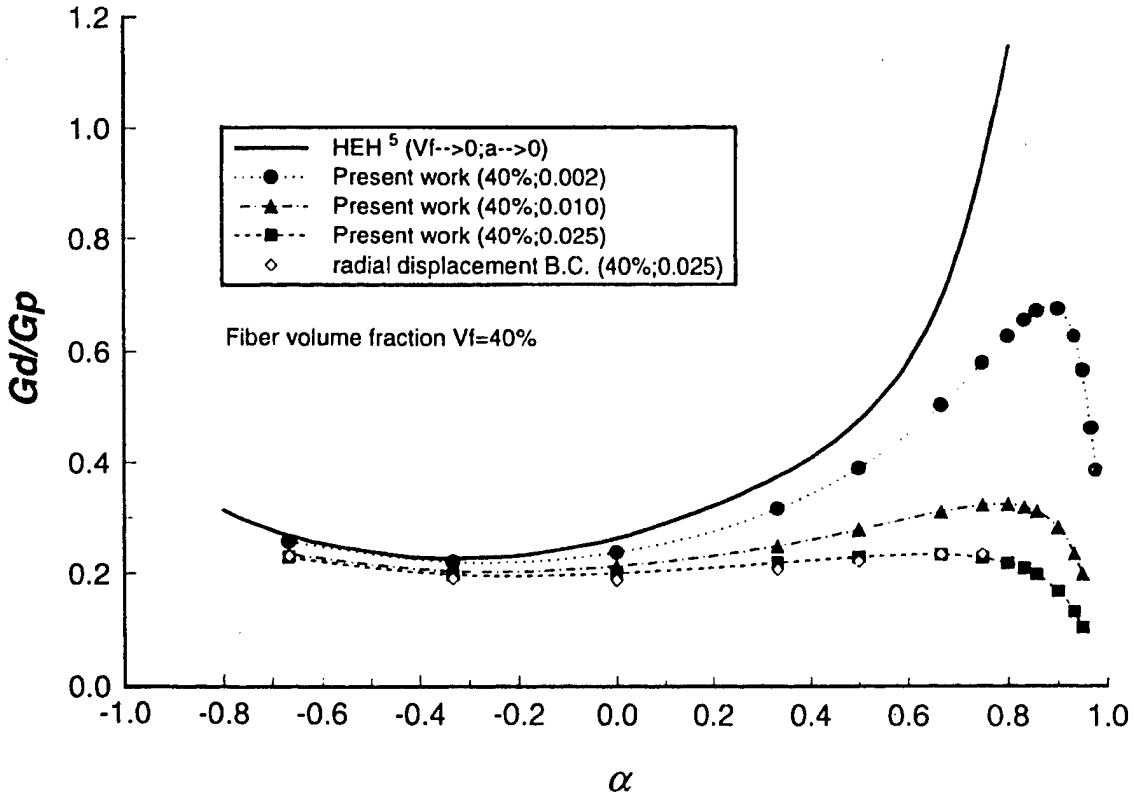

Figure 2. G_d/G_p vs. α; deflection occurs if $\Gamma_i/\Gamma_f > G_d/G_p$

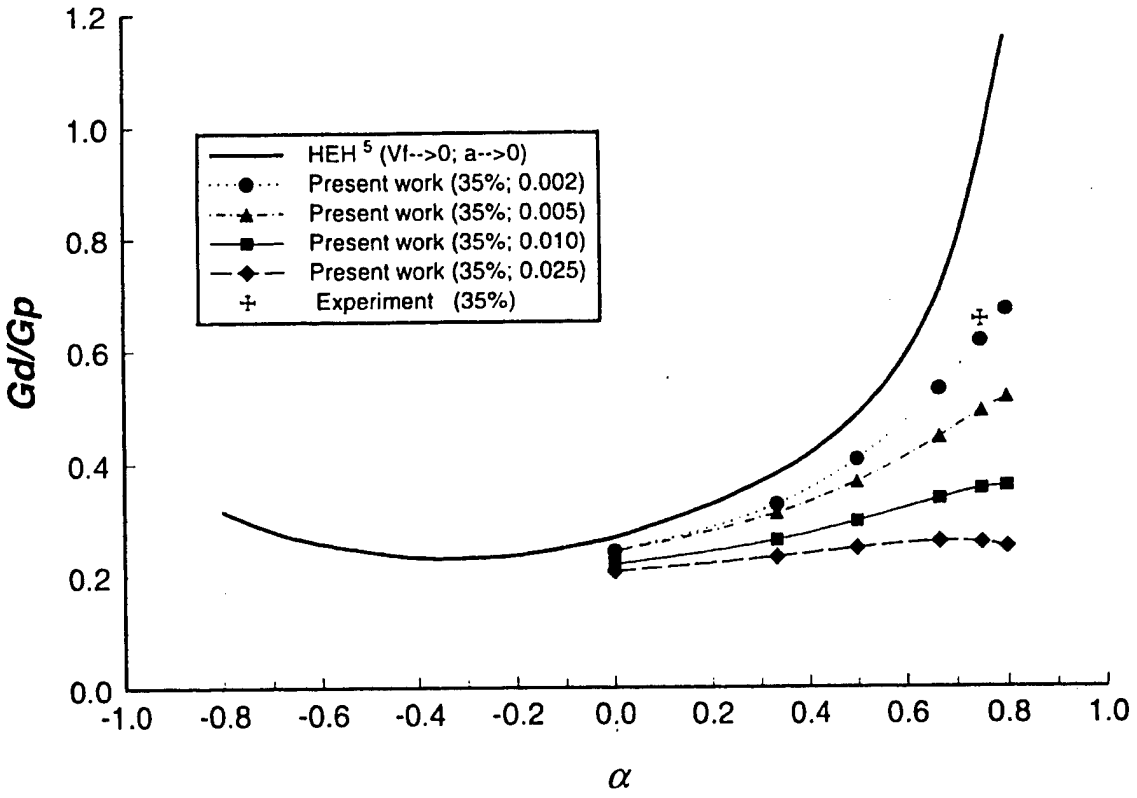

Figure 3. G_d/G_p vs. α; deflection occurs if $\Gamma_i/\Gamma_f > G_d/G_p$. Experimental data for Γ_i/Γ_f shown as +.

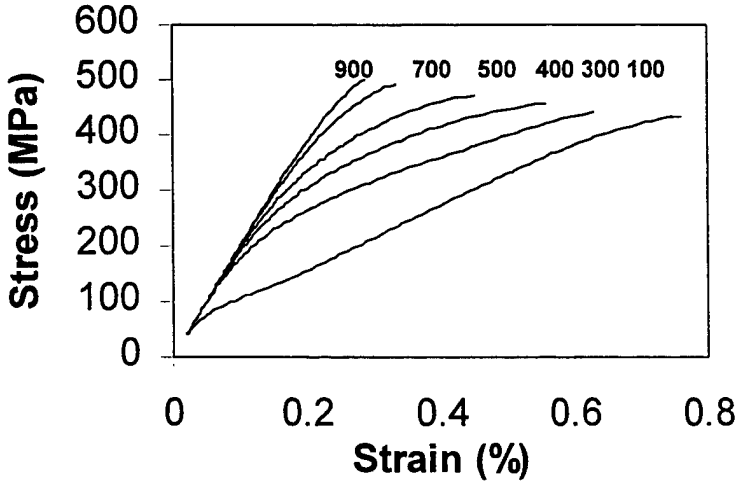

Figure 4. Stress-strain behavior versus characteristic matrix strength. Note the decreasing failure strain with increasing matrix strength.

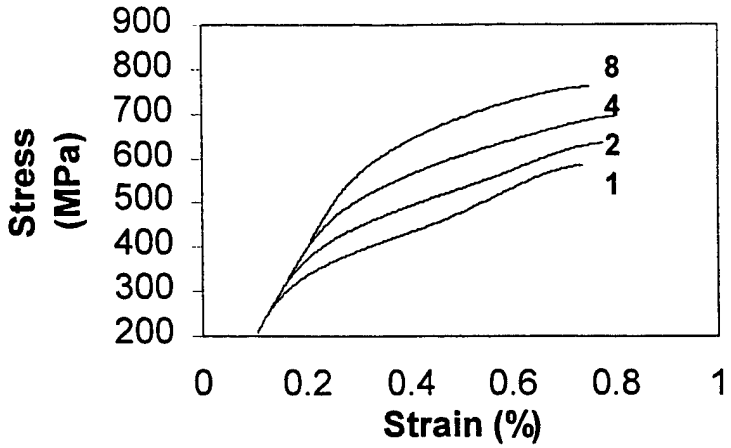

Figure 5. Predicted stress-strain behavior for interfacial τ varying by factors of 2, 4, and 8 from a baseline value. All constituent fiber and matrix properties are unchanged.

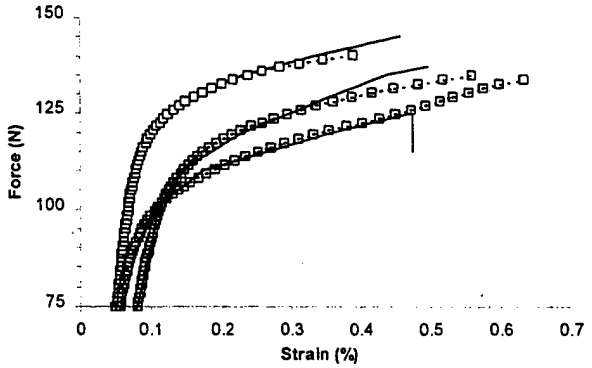

Figure 6. Predicted (symbols) and measured (solid lines) stress-strain behavior for SiC/SiC minicomposites.

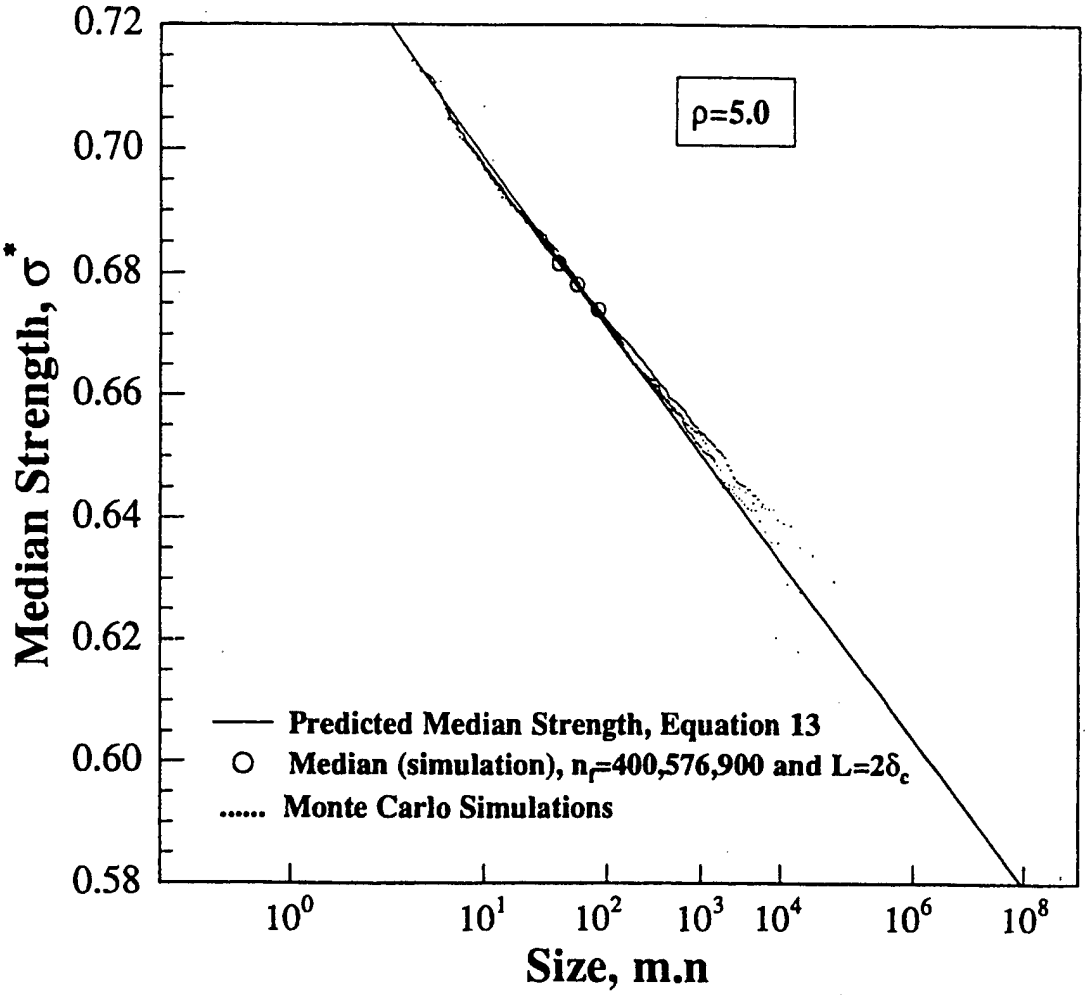

Figure 7. Median composite strength versus dimensionless composite size, as predicted by the analytic model and as measured in simulations, for fiber Weibull modulus of 5.

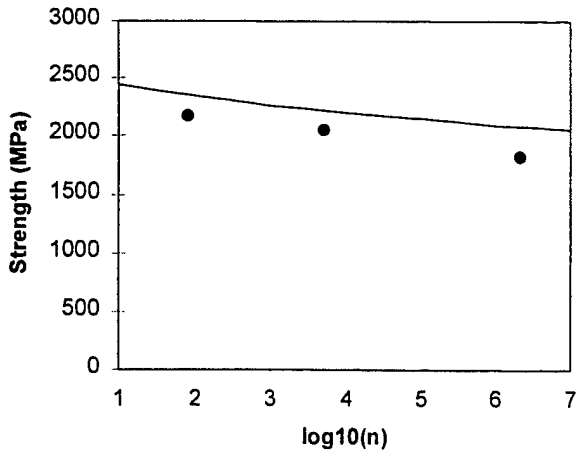

Figure 8. Predicted (solid line) and measured (points) strength of Al/Al_2O_3 composites versus dimensionless size (after Ramamurty et al.).